

TREND AND VARIABILITY OF AEROSOL OPTICAL DEPTH AT UV WAVELENGTH (340 NM) OVER ILORIN AERONET SITE IN THE NORTH CENTRAL STATE OF NIGERIA

¹Ibrahim, B. B., ²Sharafa, S. B. & ¹Usman A.

¹Department of Science Laboratory Technology, Physics/Electronics Unit, Kwara State Polytechnic, Ilorin

²Department of Physics, Usman Danfodiyo University Sokoto, Sokoto, Nigeria.

Email: ibb_fulani@yahoo.com

Phone: +2347063401453.

Abstract

Aerosol are small solid or fluid airborne mass, or particles, that remain suspended in the air and move with the motion of the air within broad limits. The extinction of sunlight reaching the ground by a vertical column of atmosphere due to aerosol is often termed as aerosol optical depth. This research work investigates the trend of Aerosol Optical Depth (AOD) at 340 nm and its variability over 13 years (2002-2014) using AERONET data for Ilorin, Nigeria. Daily and monthly mean, maximum, minimum and range of AOD values and their trends were investigated using regression analysis. The result shows that on annual basis, the minimum value of daily AOD occurred in year 2008 with a value of 0.096 in August while the maximum value of AOD occurred in 2006 with a value of 3.878. The highest range of AOD also occurred in year 2006 with a value of 3.663 in March. On year by year monthly average, the minimum value of AOD occurred in year 2008 with a value of 0.293 in August while the maximum occurred in year 2007 with a value of 1.6747 in January. Year 2008 has the highest value of range with a value of 1.3068. The result further shows that the yearly representation of daily mean, maximum, minimum and range behave similarly in trend with AOD rising from November up to March of the following year. There is a drop in AOD in May until a minimum in August of the year before another rise in the value. A quadratic fit best described the plot of daily mean, maximum, minimum and range of AOD with days of the year. AOD shows positive and negative value of monthly trend throughout the study period. No year with similar monthly trend. This analysis will be useful for Air quality assessment studies.

Keywords: Aerosol, Aerosol Optical Depth, UV, AERONET, Irradiance.

Introduction

Aerosols are tiny solid or liquid phase particles in the atmosphere. They can be naturally occurring from volcanoes, windblown dust, dust storms, forest and grassland fires, living vegetation and sea spray. They could also be anthropogenic, generated from the burning of fossil fuels (Guido & Artificio, 2016; Bassani & Cuevas-agulló, 2016; Kambezidis, 2016; Szkop & Posyniak, 2016). These aerosols occur over a wide range of sizes, extending from 10-20 μm to about $10^2 \mu\text{m}$. Aerosol particles larger than about 1 μm in size are produced by windblown dust and sea spray and bursting bubbles. Aerosols smaller than 1 μm are mostly formed by condensation process such as conversion of sulfur dioxide (SO_2) gas (released from volcanic eruptions) to sulfate particles and by formation of soot and smoke during burning processes (Mehta & Singh, 2018; Rupakheti *et al.*, 2019; Shah *et al.*, 2019). These aerosols perform a substantial role not only in the atmosphere and its processes, but also in people's health and welfare around the world (Ali *et al.*, 2015; Tang & Wang, 2016).

The seasonal variability of the aerosol optical properties and the regional Radiative Forcing (RF) are mainly controlled by aerosol loading, in which dusts have been playing an important role in the atmosphere (Falaiye *et al.*, 2013; Ginoux & Hsu, 2010; Nwofor, 2010a; Nwofor, 2010b; Ogunjobi, 2012). Atmospheric deposition is estimated to provide 450 Tg yr^{-1} of dust to the oceans (Bassani *et al.*, 2016; Kambezidis, 2016; Szkop *et al.*, 2016). Almost half of this estimated global dust input is provided by the arid regions of the Sahara and Sahel deserts resulting in a westward flow of material over the North Atlantic Ocean (Boiyo *et al.*, 2018; Guido & Artificio, 2016; Péré *et al.*, 2018). Atmospheric dust deposition is an important source of vital and limiting nutrients and metals to the ocean, affecting the oceanic carbon uptake, phytoplankton growth and productivity. Recent reports

also suggest that dust inputs may promote nitrogen fixation by providing iron and other trace metals (Nwofor & Chineke, 2007; Sharafa *et al.*, 2020).

The solar ultraviolet radiation reaching the Earth's surface has been broadly discussed during the last decades because of its biological and photochemical activity (Reinart & Veismann, 2001). Great emphasis has been placed on the potential increase in surface UV radiation due to the depletion of stratospheric ozone. Besides ozone, other atmospheric components like clouds, gaseous absorbers and tropospheric aerosols influence the transmission of UV radiation through the atmosphere (Baba *et al.*, 2015; Kumaret *et al.*, 2014; Szkop, 2016). The importance of the influence of aerosols on the surface UV radiation was introduced by Liu *et al.* (1991).

Several studies demonstrate that UV-B transmission through the atmosphere, as well as the surface UV irradiance are negatively correlated with aerosol optical depth(AOD)(Aswini *et al.*; 2018). Based on long-term sequences of AOD, Emeter & Akinyemi (2017) found that a 10% increase of AOD exhibits itself in about a 1.5% decrease in the daily erythemal UV dose and that extreme values of AOD were associated with changes in erythemal UV doses of 20–30%. Rupakheti *et al.* (2019) found that over certain parts of the Earth with a high loading of absorbing particles, the aerosols could reduce the UV flux at the surface by more than 50%. Emeter *et al.* (2015) estimated that changes in aerosol loading could give larger variations in the surface UV radiation than changes in the ozone column. Based on the effects of UV radiation on both human and plants, this paper study the trend and variability of the effects of both scattering and absorption of incoming UV radiation by atmospheric aerosol using AERONET data..

Materials and Method

Description of the Study Area

The research site is located at University of Ilorin, Nigeria. Ilorin (8.50N, 4.50E, 375m) is situated in the Guinea Savannah zone of West Africa; a transition zone between the Guinea coast and Sahel West Africa. Ilorin is in the desert transition zone between the Sahara and the savanna of upper Nigeria and is influenced by the dusty Harmattan wind (Ginoux *et al.*, 2010). Precisely, Ilorin is located at the upper tip of the guinea-savanna zone with a mean monthly average temperature of about 30.2 OC and average annual rainfall of about 873 mm(Falaiye *et al.*, 2013). Figure 1shows (a) the map of Nigeria, (b) map of Ilorin and (c) map of the site respectively.

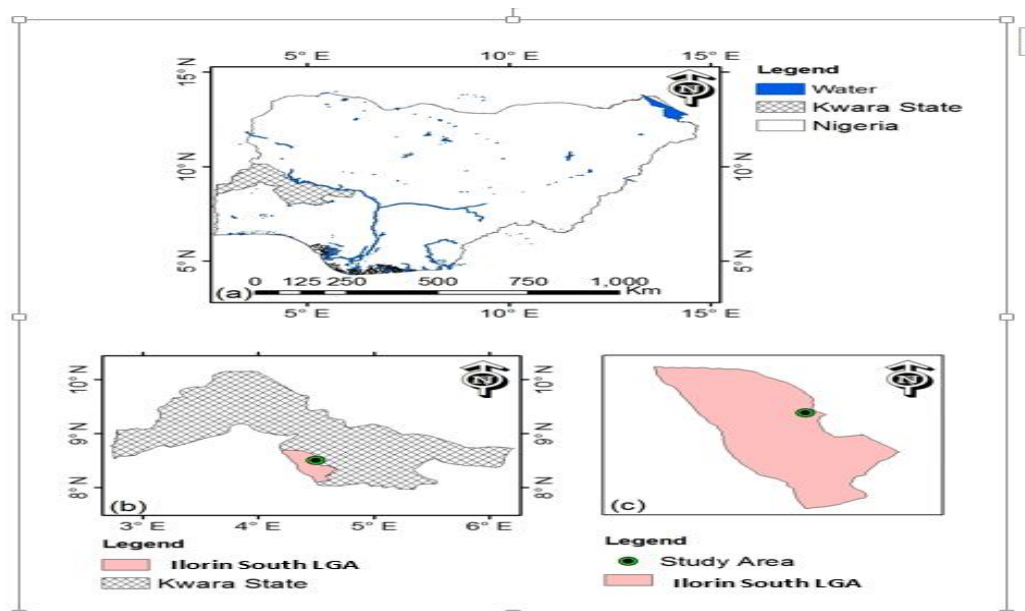


Figure 1: Digitized (a) Map of Nigeria showing Kwara State (b) Map of Kwara State showing Ilorin South LGA (c) Map of Ilorin South LGA showing study area

Instrumentation (Cimel Sun Photometer and measurements)

AERONET is an acronym for AERosol Robotic NETwork which is a federated network of CIMEL Sun photometers. Since 1995, about twenty (20) stations have been installed in West Africa by the PHOTONS component of the AERONET network, with different periods and durations of observations (Dubovik *et al.*, 2010). A CIMEL Sun photometer which is an automatic sun-sky scanning filter radiometer, allowing the measurement of the direct solar irradiance at wavelengths: 340,380,440,500,675,870,940 and 1020nm. It is solar powered, hardy and robotically pointed. Data acquired were sent to the NASA Goddard space flight center using a satellite data telemetry antenna. NASA provides preliminary processing of real-time data containing the daily pattern of AOD at all operational wavelengths. The AOD data are calculated by using the ASTPwin software (Cimel Ltd. Co) for level 1.0 AOD (raw result without cloud-screen), Level 1.5 AOD (cloud-screen AOD) based on Smirnov *et al.* (2002), level 2 AOD (quality-assured data set) and Angstrom Exponent between 440 to 870 nm. The data stored in the control box microprocessor are then transmitted via the conical-shaped antenna to any of the three geosynchronous satellites GOES, METEOSTAT or GMS from where it is retransmitted to the appropriate ground station for processing and upload to the internet at <http://aeronet.gsfc.nasa.gov/> for public access. Figure 2 shows a typical AERONET CIMEL Sun-Photometer installed on the roof.



Figure 2: AERONET CIMEL Sun-photometer at block 9 of the faculty of physical science, University of Ilorin, Nigeria.

Data acquisition

A thirteen years daily average data of AOD at 340 nm spanning from 2002-2014 were obtained from the archive of the AERONET NASA website. Due to instrument failures which occurs with AERONET, several gaps spanning many days and sometimes months occur in the AOD data series for Sub-Sahel West Africa, especially Ilorin station. A 13 years centered moving average smoother was applied to the data series. This is necessary because of the data gaps. From the daily data, the daily monthly average were extracted.

Results and Discussion of Findings

Table 1 shows the statistical summary of year to year daily AOD at 340 wavelength for Ilorin for years 2002 – 2014. The lowest minimum value of the daily minimum AOD (0.095) was observed in 2008. This showed that the atmosphere is polluted throughout the period covered by the research, as a clean atmosphere will have AOD values not exceeding 0.05 (Tanet *et al.*, 2015). Also, the year with the highest value of maximum daily AOD/atmospheric pollution (AOD = 3.878) is 2006. The highest (1.166) and lowest (0.662) average daily values of AOD shows that the atmosphere in Ilorin is highly polluted.

Table 1: Summary of year by year daily statistical AOD at 340 nm parameters for Ilorin from 2002-2014

YEAR	MIN	MAX	MEAN	MODE	STD. DEV.	RANGE
2002	0.213	2.250	0.664	0.213	0.409	2.036
2003	0.155	3.016	0.993	0.155	0.572	2.860
2004	0.303	1.858	0.864	0.371	0.371	1.555
2005	0.148	2.533	0.846	0.148	0.446	2.385
2006	0.215	3.878	0.869	0.215	0.548	3.663
2007	0.103	3.312	0.876	0.103	0.540	3.209
2008	0.095	3.663	0.856	0.957	0.549	3.567
2009	0.120	2.408	0.917	0.120	0.504	2.288
2010	0.802	1.980	1.166	0.802	0.373	1.178
2011	0.167	1.627	0.662	0.167	0.363	1.460
2012	0.156	3.632	0.908	0.156	0.611	3.476
2013	0.138	1.834	0.725	0.138	0.378	1.695
2014	0.182	2.260	0.872	0.182	0.462	2.078

Table 2 shows the statistical summary of year to year monthly AOD for Ilorin for year 2002-2014. The lowest minimum value of the yearly monthly AOD (0.293) was observed in 2008. This observation supports suggestion that the atmosphere is polluted throughout the period covered by the research. Also, the year with the highest yearly atmospheric pollution (AOD = 1.674) is 2007. The highest (1.17) and lowest (0.618) average yearly values of AOD also supports the idea that the atmosphere in Ilorin is highly polluted.

Table 2: Summary of year by year monthly statistical AOD parameters for Ilorin from 2002-2014

YEAR	MIN	MAX	MEAN	MODE	STD. DEV.	RANGE
2002	0.416	0.881	0.618	0.416	0.241	0.472
2003	0.388	1.385	0.829	0.388	0.433	0.992
2004	0.710	1.070	0.833	0.718	0.205	0.361
2005	0.413	1.563	0.786	0.413	0.341	1.150
2006	0.403	1.458	0.819	0.403	0.353	1.056
2007	0.378	1.674	0.808	0.378	0.422	1.297
2008	0.293	1.600	0.753	0.293	0.445	1.306
2009	0.359	1.510	0.781	0.366	0.417	1.151
2010	1.070	1.311	1.17	1.07	0.123	0.241
2011	0.315	0.980	0.579	0.315	0.282	0.666
2012	0.331	1.534	0.770	0.331	0.464	1.202
2013	0.421	1.38	0.661	0.421	0.350	0.966
2014	0.424	1.408	0.737	0.424	0.370	0.984

Table 3 gives the descriptive statistics of AOD at 340 nm for wet and dry seasons. The lowest mean value of AOD (0.39) during the rainy season under the period being considered was observed in 2012. With the knowledge that AODs during the rainy season is always the lowest, the turbidity of the

atmosphere in this station has come to the fore, again. The highest maximum value of AOD (0.73) during the rainy season was observed in 2006. It was also observed that the minimum value of AOD (0.28) in this season came up in 2008.

Similarly, the lowest mean value of AOD (0.91) during the dry season under the period being considered was observed in 2013. With the knowledge that AODs during the dry season is always the highest, the turbidity of the atmosphere in this station has, again, been re-echoed. The highest maximum value of AOD (1.68) during the dry season was observed in 2007. It was also observed that the minimum value of AOD (0.49) came up in 2012.

Table 3: Descriptive statistics for the wet and dry season monthly AOD from 2002-2014

Year	Wet Season				Dry Season			
	Mean	Max	Min	Range	Mean	Max	Min	Range
2002								
2003								
2004								
2005	0.51	0.61	0.40	0.21	1.12	1.56	0.70	0.86
2006	0.56	0.73	0.42	0.31	1.16	1.46	0.77	0.69
2007	0.47	0.64	0.39	0.25	1.21	1.68	0.79	0.89
2008	0.44	0.58	0.28	0.30	1.20	1.59	0.79	0.80
2009	0.45	0.54	0.34	0.20	1.22	1.51	0.89	0.62
2010								
2011								
2012	0.39	0.43	0.33	0.10	1.17	1.54	0.49	1.05
2013	0.51	0.62	0.42	0.2	0.91	1.39	0.51	0.88
2014	0.51	0.62	0.42	0.2	1.06	1.41	0.69	0.72

Figure 3 shows the yearly representation of daily mean, maximum, minimum and range of AOD at 340 nm for Ilorin for year 2002 - 2014. All the four plots show similar trend with AOD at 340nm rising from November to December up to the January, February and March of the following year.

A quadratic fit for the mean daily AOD at 340nm with days of the year (X) gives;

$$AOD = 1.756 - 0.012X + 2.79 \times 10^{-5}X^2 \quad (1)$$

$$R^2 = 0.833, \quad SD = 0.151, \quad P < 0.0001$$

The quadratic fit for the daily average maximum AOD gives;

$$AOD = 2.789 - 0.012X + 2.79 \times 10^{-5}X^2 \quad (2)$$

$$R^2 = 0.611, \quad SD = 0.448, \quad P < 0.0001$$

Also, a quadratic fit of daily average minimum gives a good correlation coefficient of 0.7504

$$AOD = 1.112 - 0.007X + 1.765 \times 10^{-5}X^2 \quad (3)$$

$$R^2 = 0.75, \quad SD = 0.12, \quad P < 0.0001$$

while the daily average range gives a weak correlation coefficient of 0.3675 with quadratic fit below:

$$AOD = 1.68 - 0.0113X + 2.63 \times 10^{-5}X^2 \quad (4)$$

$$R^2 = 0.367, \quad SD = 2.12, \quad P < 0.0001$$

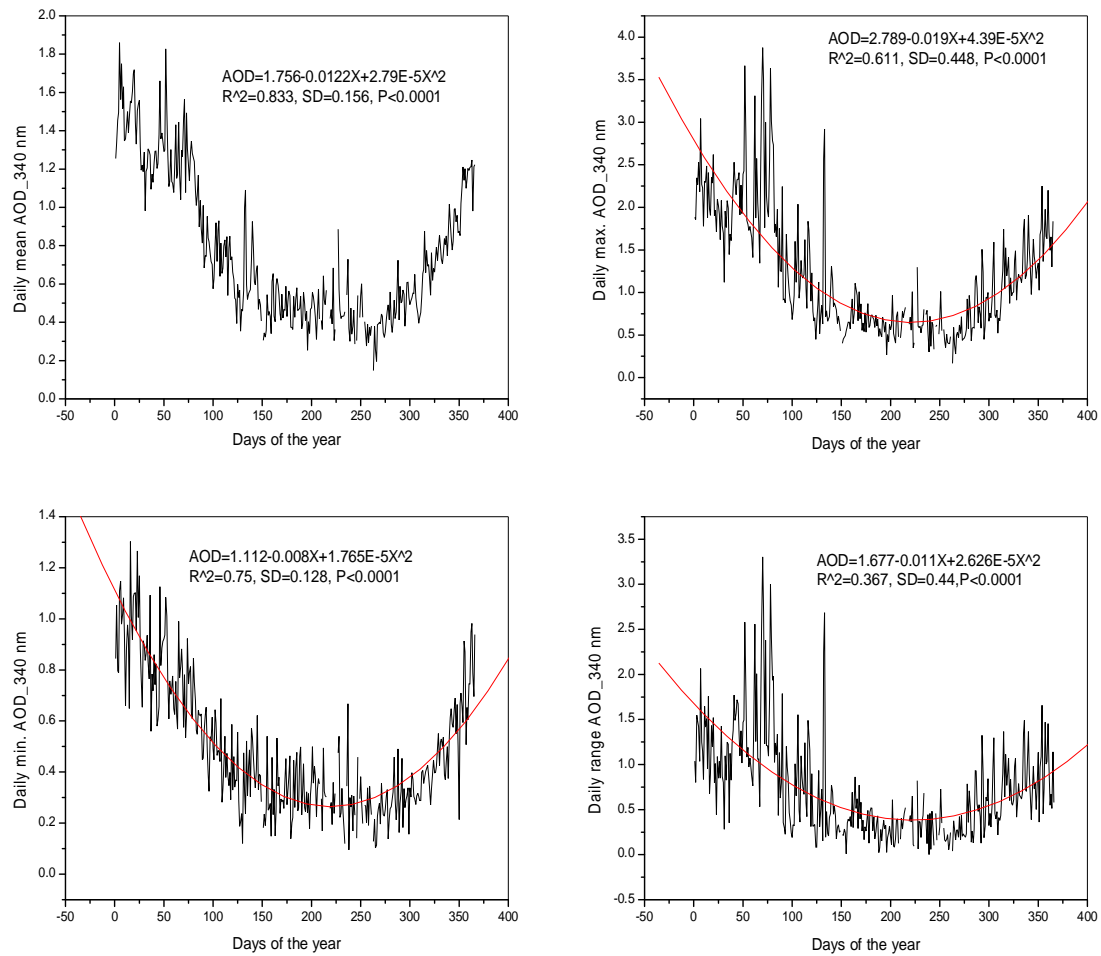


Figure 3: Fit for the variation of yearly representation of Daily mean, maximum, minimum, and range for AOD at 340 nm for Ilorin for year 2002-2014.

Figure 4 shows the plots of monthly mean, maximum, minimum and range of AOD in Ilorin for year 2002 – 2014 respectively. All four plots have similar trend except for the range. The mean, maximum and minimum monthly AOD have the best correlation coefficients of 0.934, 0.921 and 0.962 respectively with months of the year. Monthly range of AOD at 340 nm has a fairly good correlation coefficient of 0.518 with months of the year.

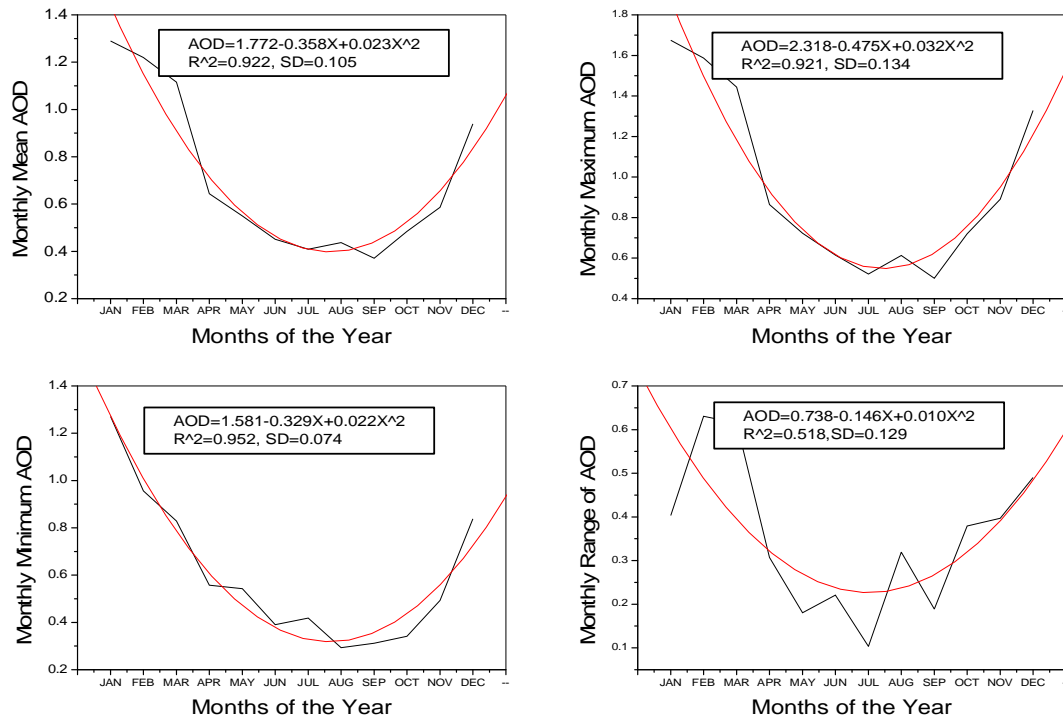


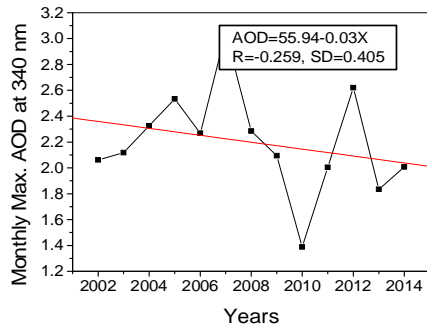
Figure 4: Fit for the variation of monthly mean, maximum, minimum and range of daily mean AOD at 340 nm for Ilorin for year 2002-2014.

The quadratic fit of the form $y = ax^2 + bx + c$ for the four parameters are presented in Table 4.

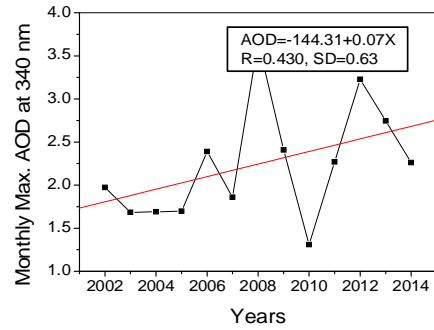
Table 4: Quadratic fits and statistical errors

AOD at 340nm	Constants			Standard Deviation (SD)	P
	A	b	c		
Average monthly mean	0.023	-0.358	1.772	0.105	< 0.0001
Average Monthly Maximum	0.032	-0.475	2.320	0.134	< 0.0001
Average Monthly Minimum	0.022	-0.330	1.581	0.074	< 0.0001
Average Monthly Range	0.010	-0.145	0.740	0.129	= 0.037

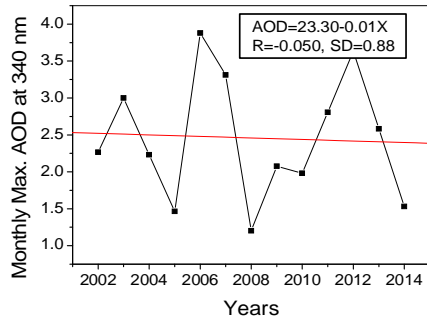
Figure 5 (a)-(l) shows the linear regression trends in monthly maximum behaviour of AOD from year 2002-2014 starting from January to December for all the years. This approach was used by Abdou, (2014) to study the temperature trend in Mekkah. The monthly maximum shows both increasing and decreasing trends with annual rate of decrease to be -0.030 for January. Month of February shows an increasing rate of 0.0729 , this is followed by another decreasing and increasing rate of -0.0104 and 0.0143 for March and April respectively. The months of May, June, August, September, November and December show a decreasing trend of AOD for Ilorin with decreasing rate of -0.047 , -0.0084 , -0.0085 , -0.0134 , 0.040 and -0.059 respectively, while July and October show an increasing rate of 0.0081 and 0.0047 respectively. This implies that the aerosol loading in the months of February, April, July and October increase by 0.949 , 0.182 , 0.104 and 0.065 respectively and decreases in the months of January, March, June, August and December by -0.91 , -0.130 , -0.611 , -0.104 , -0.117 , -0.167 , -0.52 and -0.767 respectively for the 13 years considered. The linear regression summary is shown in Table 5 which shows the regression equation and correlation coefficient.



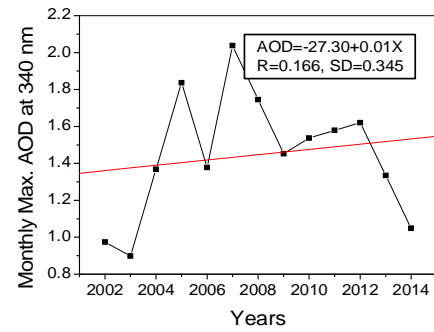
(a) January



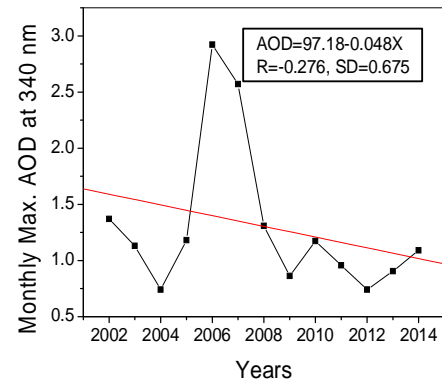
(b) February



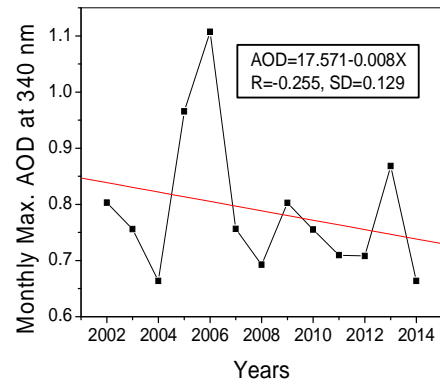
(c) March



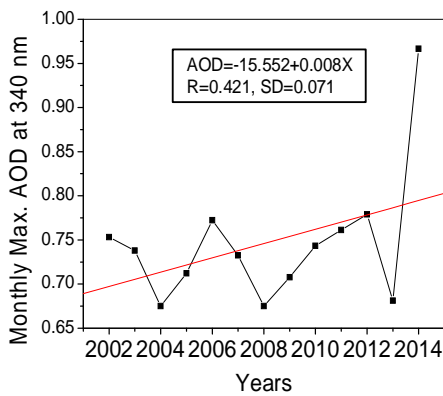
(d) April



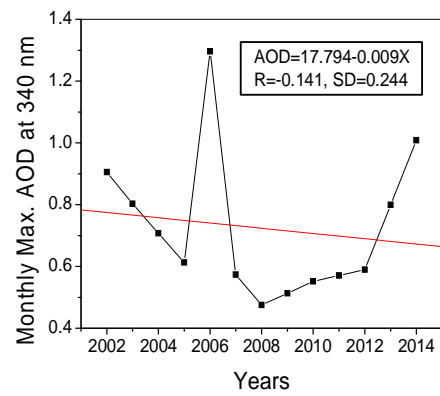
(e) May



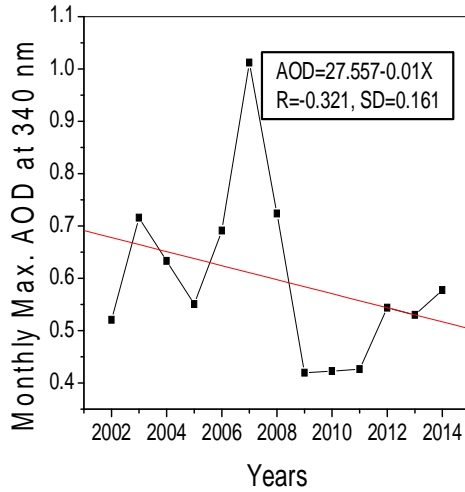
(f) June



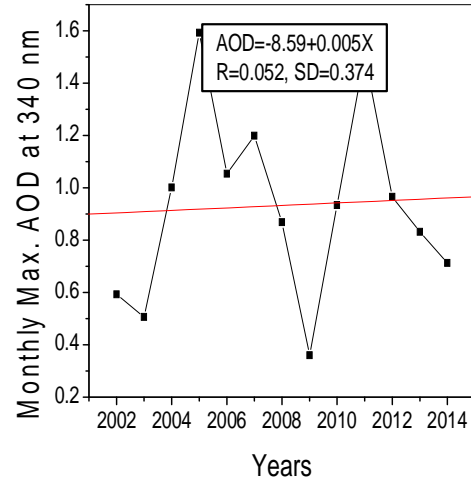
(g) July



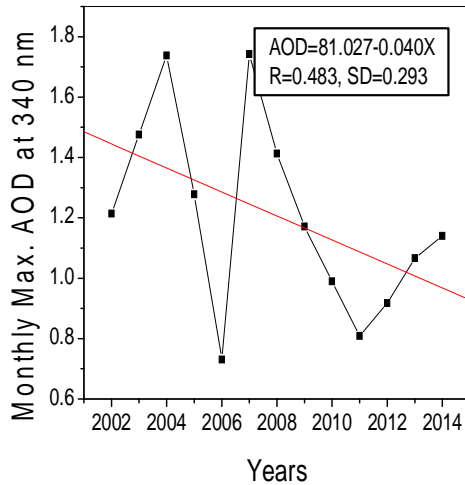
(h) August



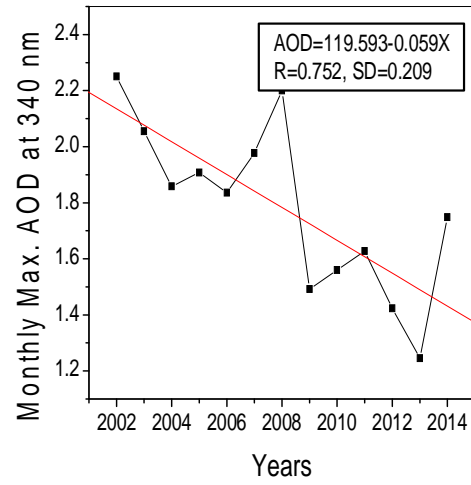
(i) September



(j) October



(k) November



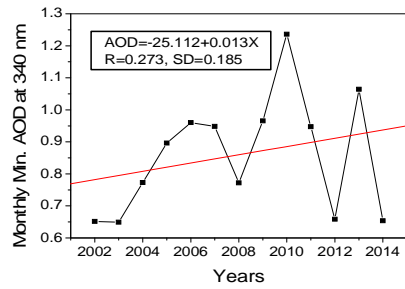
(l) December

Figure 5 (a)-(l): Linear regression trends of monthly maximum of yearly AOD at 340 nm at Ilorin from January to December for 2002-2014.

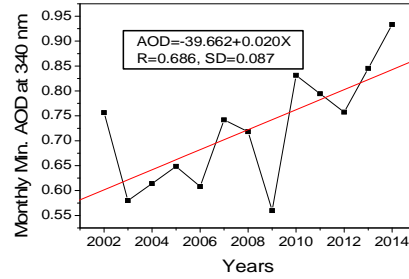
Table 5: Linear regression equation of the monthly maximum of AOD.

Months	Regression Equation	R	Months	Regression Equation	R
Jan	$Y=55.94-0.07X$	0.259	Jul	$Y=15.55+0.008X$	0.421
Feb	$Y=144.3+0.073X$	0.428	Aug	$Y=17.79-0.009X$	0.141
Mar	$Y=23.13-0.01X$	0.08	Sep	$Y=27.0-0.013X$	0.321
Apr	$Y=27.3+0.014X$	0.155	Oct	$Y=8.55+0.005X$	0.051
May	$Y=67.13-0.048X$	0.078	Nov	$Y=81.02-0.04X$	0.403
Jun	$Y=17.57-0.008X$	0.255	Dec	$Y=119.59-0.05X$	0.752

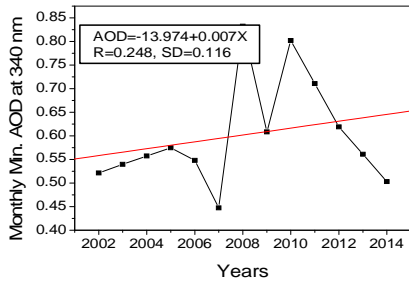
Figure 6 (a)-(l) shows the linear regression trends in the monthly minimum of yearly AOD at 340 nm for Ilorin from January to December (2002-2014).



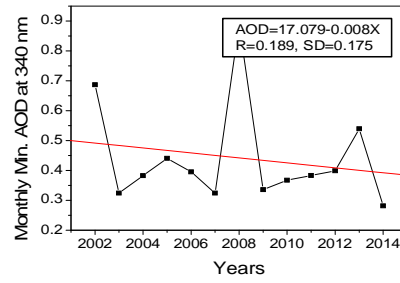
(a) January



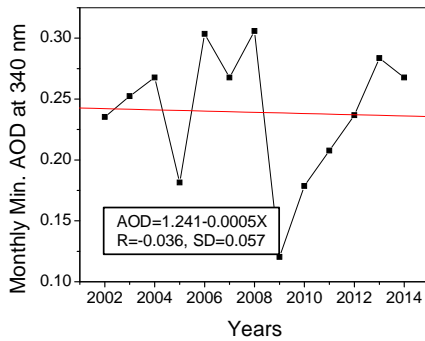
(b) February



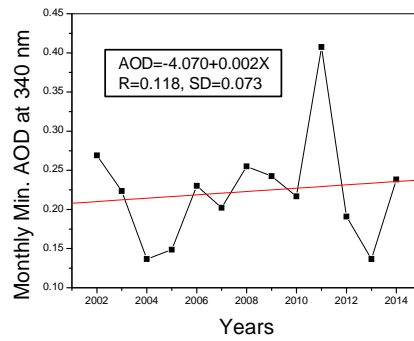
(c) March



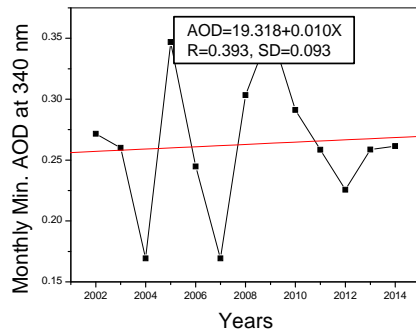
(d) April



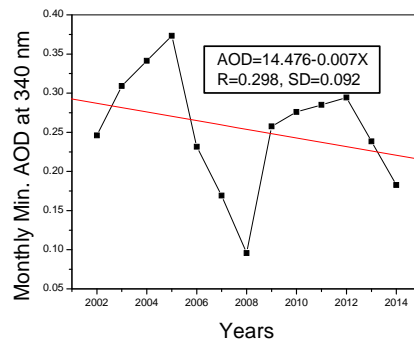
(e) May



(f) June



(g) July



(h) August

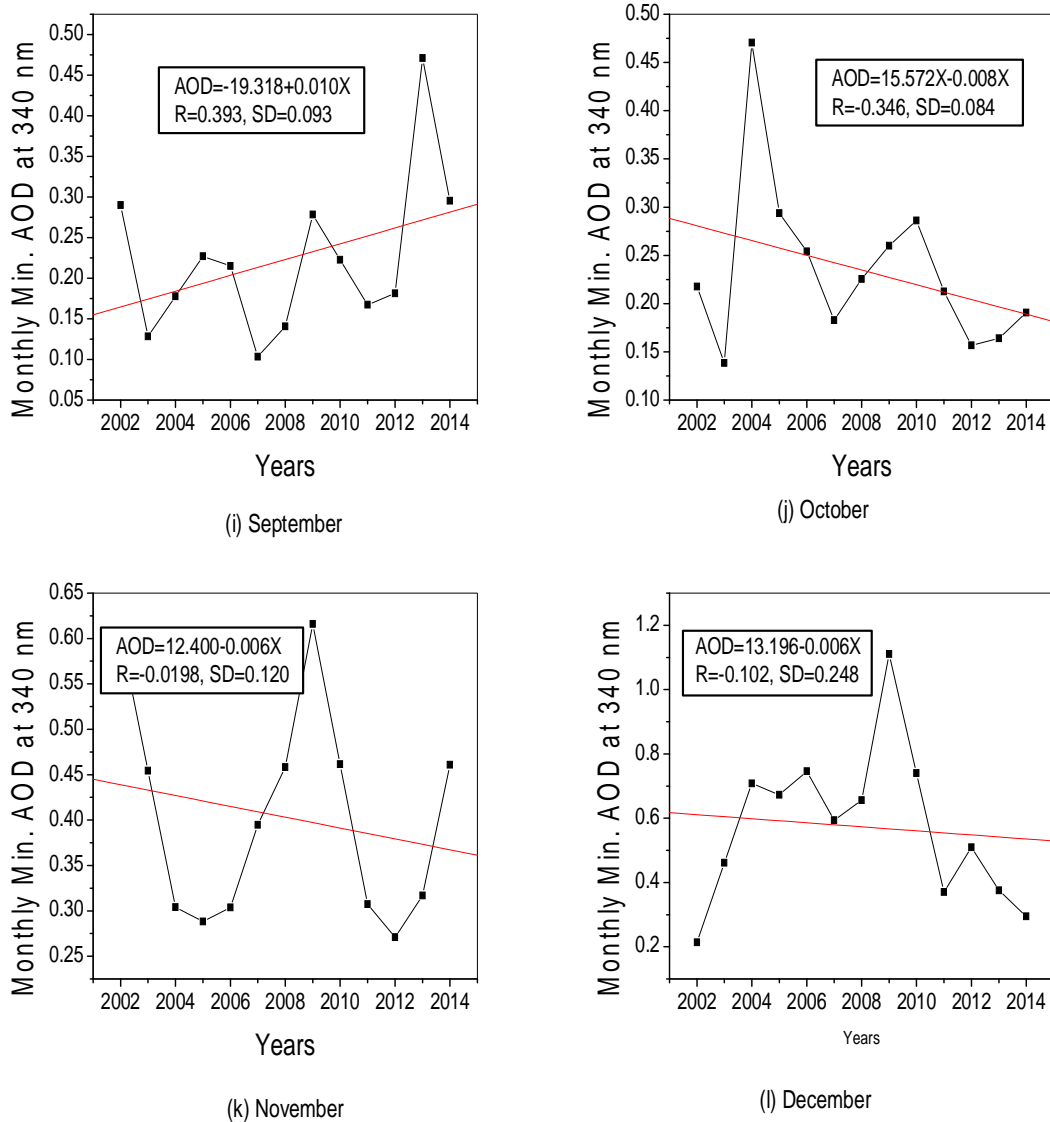


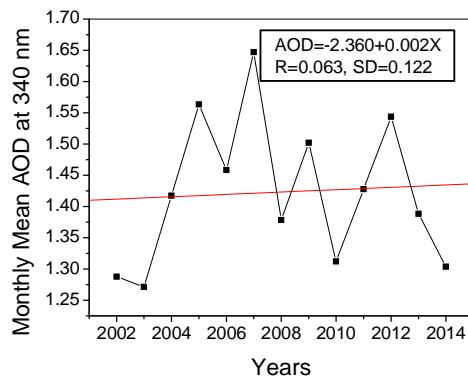
Figure 6 (a)-(b): Linear regression trends of monthly minimum of yearly AOD at 340 nm at Ilorin from January to December for 2002-2014.

There is an increase in trend of the monthly minimum of AOD for Ilorin in January, February, March, June, July and September with annual increasing rate of 0.0129, 0.0201, 0.007, 0.0021, 9.48×10^{-4} and 0.0097 respectively while annual decreasing rate of -0.080 , -4.99×10^{-4} , -0.008 , -0.007 , -0.0055 and -0.006 respectively for April, May, August, October, November and December. This means that for the 13 years considered, AOD in January, February, March, June and September increases by 0.169, 0.26, 0.091 and 0.13 respectively and decreases in April, May, July, August, October, November and December by -1.04, -0.0052, -0.0117, -1.04, -0.091, -0.078 and -0.078 respectively. The linear regression equation for the monthly minimum AOD is shown below.

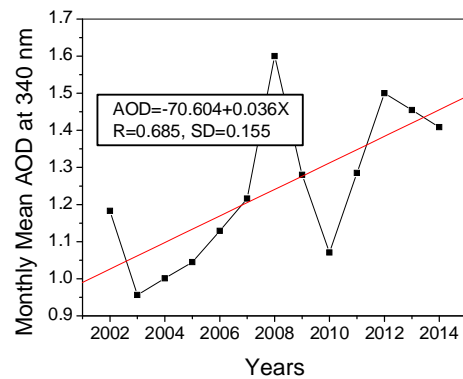
Table 6: Linear regression equation of the monthly minimum of AOD.

Months	Regression Equation	R	Months	Regression Equation	R
Jan	$Y=23.11+0.013X$	0.273	Jul	$Y=1.64-9.48E-4X$	0.058
Feb	$Y=39.08+0.02X$	0.886	Aug	$Y=11.37-0.008X$	0.291
Mar	$Y=12.97+0.007X$	0.248	Sep	$Y=19.31+0.010X$	0.393
Apr	$Y=17.0-0.008X$	0.008	Oct	$Y=14.47-0.007X$	0.293
May	$Y=1.24-4.98E-4X$	0.057	Nov	$Y=12.40-0.006X$	0.120
Jun	$Y=4.07-002X$	0.118	Dec	$Y=13.19-0.006X$	0.102

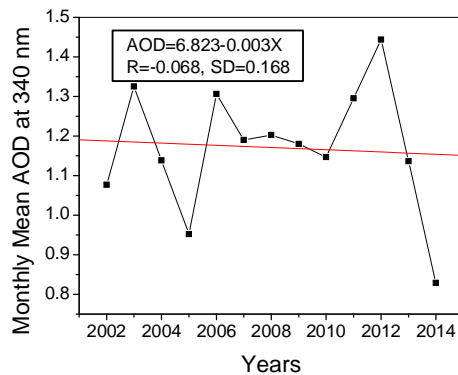
Figure 7(a)-(b) shows the monthly trend in monthly mean of yearly AOD at 340 nm for Ilorin from January to December beginning from 2002 to 2014. An increasing trend in the months of January, February, April, June, July and September with annual increasing rate of 0.0018 , 0.357 , 9.71×10^{-4} , 0.001 , 5.58×10^{-4} , and 6.26×10^{-4} respectively. Decreasing trend was found in March, May, August, October, November and December with an annual decreasing rate of -0.0028 , -0.0042 , -0.0191 , 0.0047 , -0.031 and 0.01 respectively.



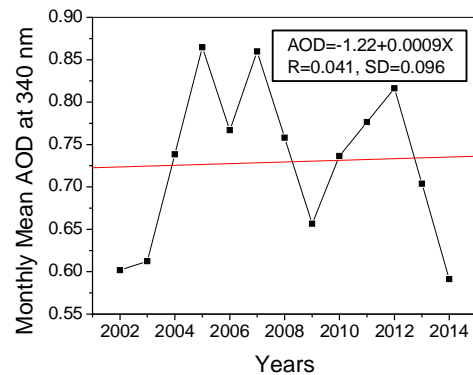
(a) January



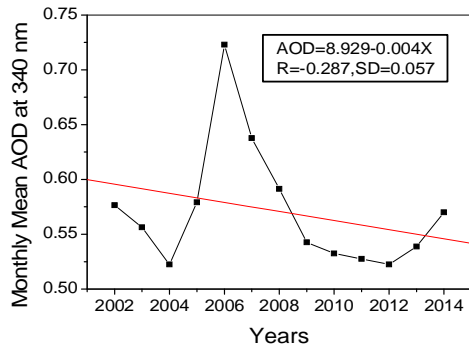
(b) February



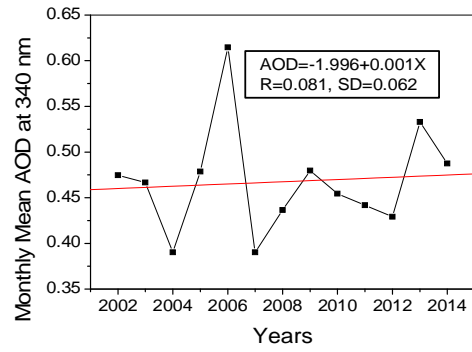
(c) March



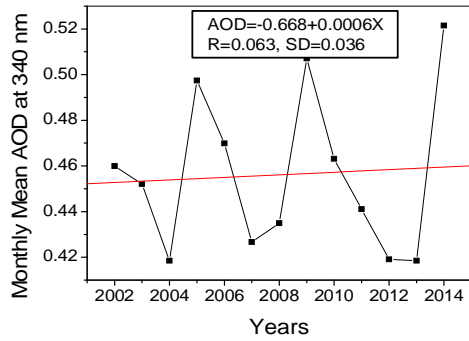
(d) April



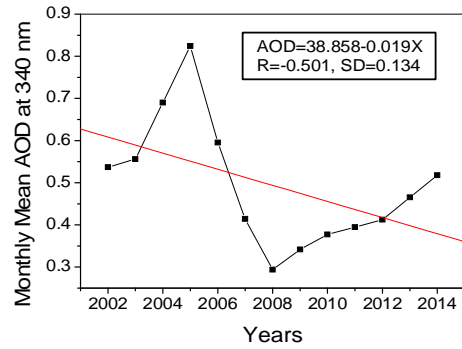
(e) May



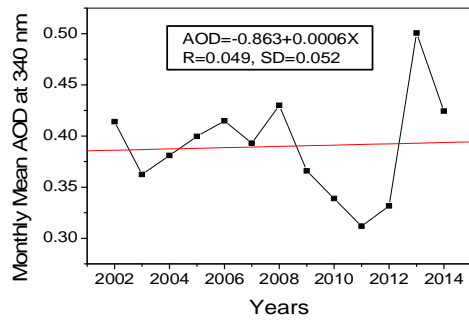
(f) June



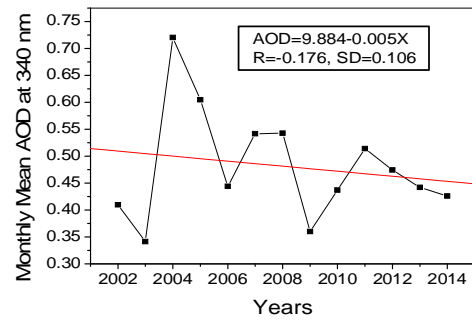
(g) July



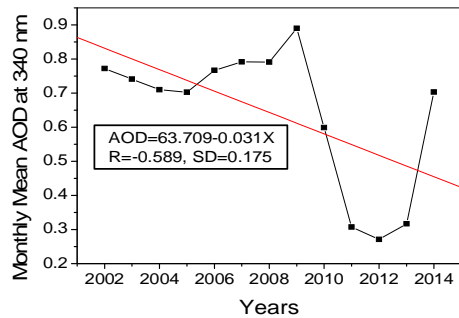
(h) August



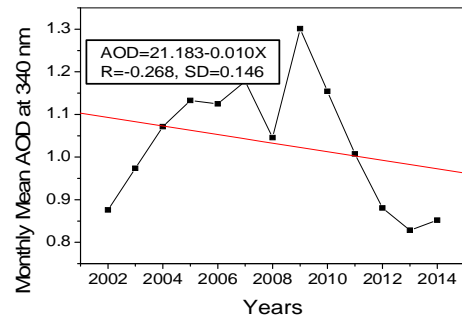
(i) September



(j) October



(k) November



(l) December

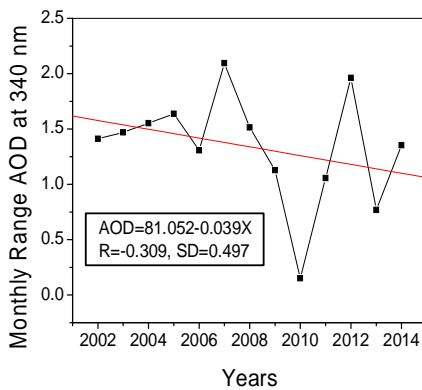
Figure 7 (a)-(l): Linear regression trends of monthly mean of yearly AOD_{340 nm} at Ilorin from January to December for 2002-2014.

This means that during January, February, April, June, September and October an increase of AOD by 0.20, 0.468, 0.0117, 0.013, 0.0065, 0.0078 and 0.065 was noticed. Also, a decrease in the months of March, May, August, November and December for the 13 years period was observed. The linear regression summary for the monthly mean of AOD is shown in Table 7

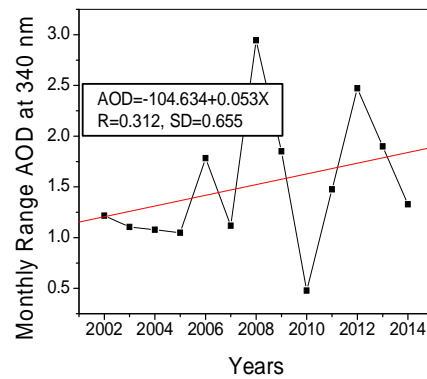
Table 7: Linear regression equation of the monthly mean of AOD.

Months	Regression Equation	R	Months	Regression Equation	R
Jan	$Y=2.36+0.02X$	0.063	Jul	$Y=0.69+5.58E-4X$	0.063
Feb	$Y=70.60+0.036X$	0.625	Aug	$Y=38.85-0.019X$	0.501
Mar	$Y=6.82-0.003X$	0.058	Sep	$Y=0.87+6.26E-4X$	0.049
Apr	$Y=1.22+9.71E-4X$	0.041	Oct	$Y=9.88-0.005X$	0.176
May	$Y=8.93-0.004X$	0.289	Nov	$Y=63.71-0.031X$	0.589
Jun	$Y=1.99+0.01X$	0.081	Dec	$Y=21.18-0.010X$	0.258

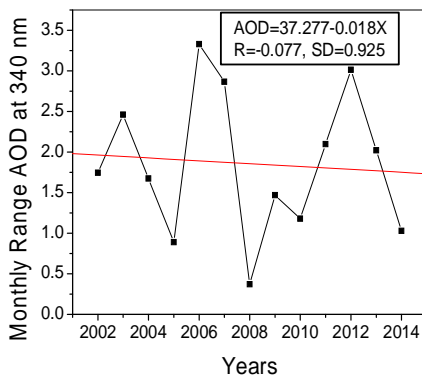
Figure 8(a)-(l) depicts the linear regression trends of monthly range of yearly mean AOD at 340 nm for Ilorin also from January to December (2002-2014).



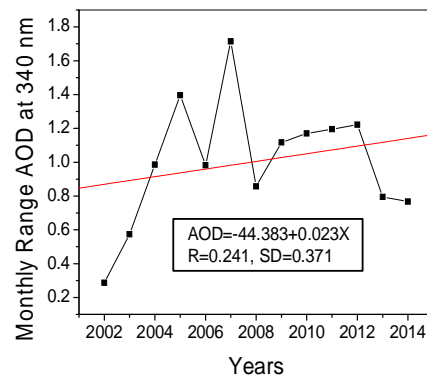
(a) January



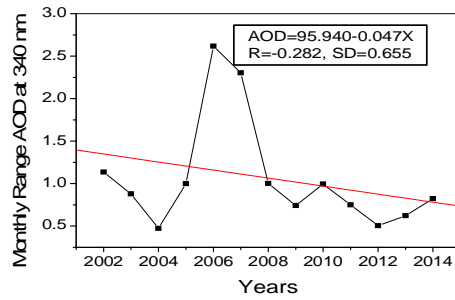
(b) February



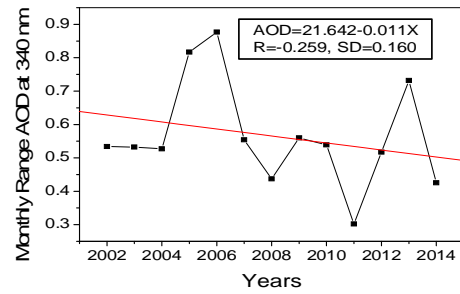
(c) March



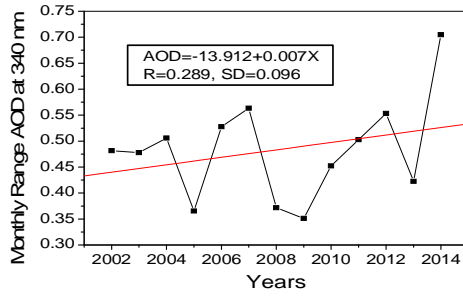
(d) April



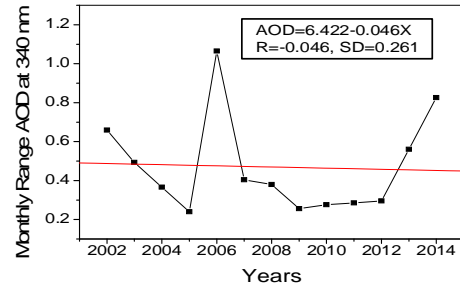
(e) May



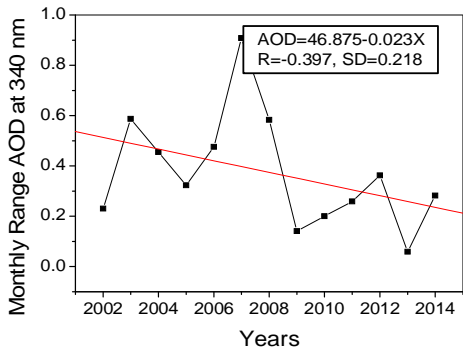
(f) June



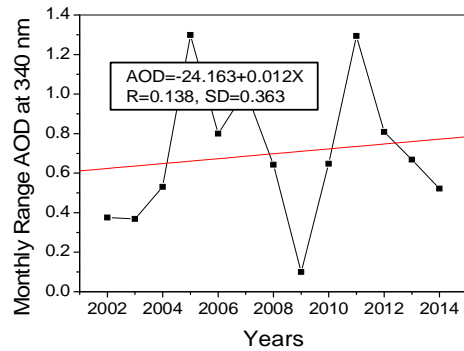
(g) July



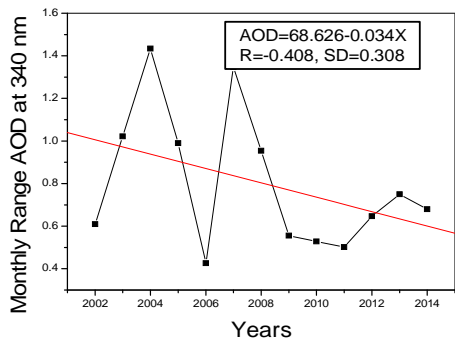
(h) August



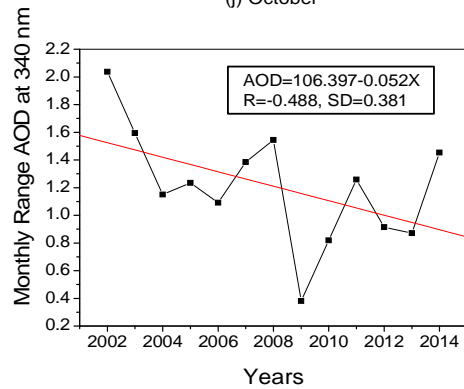
(i) September



(j) October



(k) November



(l) December

Figure 8 (a)-(l): Linear regression trends of monthly range of yearly AOD_{340 nm} at Ilorin from 2002-2014.

This means that there is a negative annual regression rate in January, March, May, June, August, September, November and December with decreasing rate of -0.0397, -0.0176, -0.047, -0.011, -0.003, -0.023, -0.034, and -0.053 respectively while the annual increment rate of 0.053, 0.023, 0.007, and 0.012 for February, April, July and October respectively was observed. The AOD variation rate means that for the 13 years considered, February, April, June, July, October, November and December, it increase by 0.039, 0.156, 0.013, 1.495, 0.169, 0.143 and 0.143 respectively and decreases in January, March, May, August and September by -0.247, -0.026, -0.117, -0.052 and -0.039 respectively. The linear regression summary of monthly range of AOD and the correlation coefficient is shown below:

Table 8: Linear regression equation of the monthly range of AOD.

Months	Regression Equation	R	Months	Regression Equation	R
Jan	$Y=61.05-0.04X$	0.309	Jul	$Y=13.91+0.007X$	0.283
Feb	$Y=104.64+0.053X$	0.312	Aug	$Y=6.42-0.003X$	0.076
Mar	$Y=67.28-0.018X$	0.077	Sep	$Y=46.88-0.023X$	0.397
Apr	$Y=44.33+0.023X$	0.241	Oct	$Y=24.16+0.138X$	0.138
May	$Y=95.94-0.047X$	0.282	Nov	$Y=68.52-0.034X$	0.408
Jun	$Y=21.64-0.011X$	0.258	Dec	$Y=106.39-0.052X$	0.448

Conclusion and Recommendation

The analysis shows that there are both positive and negative trend on monthly variations of the mean, maximum, minimum and range of values of AOD during the period of study. On the seasonal basis, highest mean AOD for wet season (0.56) occurred in year 2006. The peak maximum value was 0.73, largest minimum and range were found to be 0.42 and 0.31 in year 2006 respectively. During the dry season, highest mean (1.22) of AOD was observed in year 2009, highest maximum (1.68) was in year 2007 and highest minimum (0.79) was in year 2007 and 2008. The highest range of AOD for dry season (0.89) is in the year 2007. The increasing and decreasing trend of AOD has some implications on both plant and animal. If AOD is high, there will be more dust in the atmosphere, tree leaves falling, dryness in plants and skin dryness in animal. Human beings are prone to catarrh, cough and prevailing air borne diseases. On the other hand, if AOD is low, flooding is experienced and cattle herders would start coming from the northern Nigeria and green leaf would start coming up on the tree. The research recommends that study should be extended to AOD at other wavelengths in the study area. The AERONET AOD data of the study area should be compared with other stations in West Africa and whole Africa at large.

References

- Abdou, A. E. A. (2014). Temperature Trend on Makkah, Saudi Arabia. *Atmospheric and Climate Sciences*, 4, 457–481.
- Ali, A., Assiri, M., Shahid, S., & Dambul, R. (2015). MODIS Dark Target and Deep Blue aerosol optical depth validation over Bangladesh. *Malaysian Journal of Space*, 11(11), 74–83.

- Aswini, A. R., Hegde, P., & Nair, P. R. (2018). Carbonaceous and inorganic aerosols over a sub-urban site in peninsular India: Temporal variability and source characteristics. *Atmospheric Research*, 199(1), 40–53. <https://doi.org/10.1016/j.atmosres.2017.09.005>
- Baba, H., Kannemadugu, S., Varghese, A. O., Mukkara, S. R., Joshi, A. K., & Moharil, S. V. (2015). Discrimination of Aerosol Types and Validation of MODIS Aerosol and Water Vapour Products Using a Sun Photometer over Central India. *Aerosol and Air Quality Research*, 15(1), 682–693. <https://doi.org/10.4209/aaqr.2014.04.0088>
- Bassani, C., Manzo, C., Zakey, A., & Cuevas-agulló, E. (2016). Effect of the Aerosol Type Selection for the Retrieval of Shortwave Ground Net Radiation: Case Study Using Landsat 8 Data. *Atmosphere*, 7(111), 2–17. <https://doi.org/10.3390/atmos7090111>
- Boiyo, R., Kumar, K. R., & Zhao, T. (2018). Optical , microphysical and radiative properties of aerosols over a tropical rural site in Kenya , East Africa: Source identification , modification and aerosol type discrimination Optical , microphysical and radiative properties of aerosols over a tropi. *Atmospheric Environment*, 177(1), 234–252. <https://doi.org/10.1016/j.atmosenv.2018.01.018>
- Dubovik, O., Smirnov, A., Holben, B. N., King, M. D., Kaufman, Y. J., & Slutsker, I. (2010). Accuracy assessments of aerosol optical properties retrieved from AERONET sun and sky radiance measurements. *Journal of Geophysical Research*, 105(1), 9791–9806.
- Emetere, M. E., & Akinyemi, M. L. (2017). A short review on the effects of aerosols on visibility impairment. *Short Review*, 1(1), 6–11.
- Emetere, M. E., Akinyemi, M. L., & Akin-Ojo, O. (2015). Parametric retrieval model for estimating aerosol size distribution via the AERONET, LAGOS station. *Environmental Pollution*, 207(1), 381–390. <https://doi.org/10.1016/j.envpol.2015.09.047>
- Falaiye, O., Yakubu, A., Aweda, F., & Abimbola, O. (2013). Mineralogical characteristics of harmattan dust in ilorin, sub-sahara africa. *Ife Journal of Science*, 15(1), 175–181.
- Ginoux, P., Garbuzov, D., & Hsu, N. . (2010). Identification of anthropogenic and natural dust sources using Moderate resolution Imaging Spectrometer (MODIS) deep blue level 2 data. : 5204. *Journal of Geophysical Research*, 115 (5204), 1–10. <https://doi.org/10.1029/2009JD012398>
- Guido, R. M. D., & Artificio, M. M. (2016). Aerosol Optical Thickness and Water Vapor in the Atmosphere of Metro Manila. *International Journal of Astronomy*, 5(1), 1–6.
- Kambeizidis, H. D. (2016). Aerosol climatology and discrimination of different types over Athens , Greece , based on MODIS data. *Atmospheric Environment*, 41(1), 7315–7329. <https://doi.org/10.1016/j.atmosenv.>
- Kumar, K. R., Sivakumar, V., Reddy, R. R., Gopal, K. R., & Adesina, A. J. (2014). Identification and Classification of Different Aerosol Types over a Subtropical Rural Site in Mpumalanga , South Africa: Seasonal Variations as Retrieved from the AERONET Sunphotometer. *Aerosol and Air Quality Research*, 14(1), 108–123. <https://doi.org/10.4209/aaqr.2013.03.0079>
- Liu, S. C., McKeen, S. A., & Madronich, S. (1991). Effect of anthropogenic aerosols on biologically active ultraviolet radiation. *Geophysical Research Letters*, 8, 2265–2268.
- Mehta, M., & Singh, N. (2018). Global trends of columnar and vertically distributed properties of aerosols with emphasis on dust , polluted dust and smoke - inferences from 10-year long CALIOP observations. *Remote Sensing of Environment*, 208(1), 120–132. <https://doi.org/10.1016/j.rse.2018.02.017>

- Nwofor, K., & Chineke, T. C. (2007). Mathematical representation of seasonal cycles of aerosol optical depths at ilorin nigeria using aeronet data. *Global Journal of Pure and Applied Sciences*, 13(2), 285–294.
- Nwofor, O K. (2010). Seasonal Levels of Meteorological Visibility at Port-Harcourt Nigeria and Possible Links to Aerosol Loading and Humidification . *The Pacific Journal of Science and Technology*, 11(2), 544–551.
- Nwofor, Okey K. (2010). Rising Dust Aerosol Pollution at Ilorin in the Sub-sahel Inferred from 10-year Aeronet Data: Possible Links to Persisting Drought Conditions. *Research Journal of Environmental and Sciences*, 2(4), 216–225.
- Ogunjobi, K. O., Oluleye, A., & Ajayi, V. O. (2012). A long-term record of aerosol index from TOMS observations and horizontal visibility in sub-Saharan West Africa. *International Journal of Remote Sensing*, 33(19), 6076–6093.
- Péré, J., Rivellini, L., Crumeyrolle, S., Chiapello, I., Minvielle, F., Thieuleux, F., & Choël, M. (2018). Simulation of African dust properties and radiative effects during the 2015 SHADOW campaign in Senegal. *Atmospheric Research*, 199(1), 14–28.
<https://doi.org/10.1016/j.atmosres.2017.07.027>
- Reinart, A., Vaht, M., & Veismann, U. (2001). A case study of the impact of boundary layer aerosol size distribution on the surface UV irradiance. *Atmospheric Environment*, 35(1), 5041–5051.
- Rupakheti, D., Kang, S., Bilal, M., Gong, J., & Xia, X. (2019). Aerosol optical depth climatology over Central Asian countries based on Aqua-MODIS Collection 6 . 1 data : Aerosol variations and sources. *Atmospheric Environment*, 207(1), 205–214.
<https://doi.org/10.1016/j.atmosenv.2019.03.020>
- Shah, Z., Suo, H., Liu, M., Ma, L., Alam, K., Gul, A. & Bahadar, S. (2019). Aerosol clustering in an urban environment of Beijing during (2005 – 2017). *Atmospheric Environment*, 213(1), 534–547. <https://doi.org/10.1016/j.atmosenv.2019.06.027>
- Sharafa, S. B., Aliyu, R., Ibrahim, B. B., Tijjani, B. I., Darma, T. H., Gana, U. M. & Sulu, H. T. (2020). Model Prediction and Climatology of Aerosol Optical Depth (τ_{550}) and Angstrom Exponent ($\alpha_{470-660}$) over Three Aerosol Robotic Network Stations in sub-Saharan Africa using Moderate Resolution Imaging Spectroradiometer Data. *Nigerian Journal of Technology*, 39(1), 255–268.
<https://doi.org>
- Smirnov, A., Holben, B. N., Dubovik, O., O'Neill, N. T., Eck, T. F., Westphal, D. L. & Slutsker, I. (2002). Atmospheric Aerosol Optical Properties in the Persian Gulf. *Journal of Atmospheric Science*, 59(1), 620–634.
- Szkop, A., Pietruczuk, A., & Posyniak, M. (2016). Classification of Aerosol over Central Europe by Cluster Analysis of Aerosol Columnar Optical Properties and Backward Trajectory Statistics. *Acta Geophysica*, 64(6), 2650–2676. <https://doi.org/10.1515/acgeo-2016-00112>
- Tan, F., Lim, H. S., Abdullah, K., Yoon, T. L., & Holben, B. (2015). AERONET data – based determination of aerosol types. *Atmospheric Pollution Research*, 6(1), 682–695.
<https://doi.org/10.5094/APR.2015.077>
- Tang, B., & Wang, J. (2016). A Physics-Based Method to Retrieve Land Surface Temperature From MODIS Daytime Midinfrared Data. *Geoscience and Remote Sensing*, 54(8), 4672–4679.